Available online at www.sciencedirect.com
ScienceDirect
European Journal of Medicinal Chemistry 41 (2006) 1446–1455
EUROPEAN JOURNAL OF MEDICINAL CHEMISTRY
http://www.elsevier.com/locate/ejmech

Original article

Structure-based pharmacophore of COX-2 selective inhibitors and identification of original lead compounds from 3D database searching method

Catherine Michaux [a,*], Xavier de Leval [b], Fabien Julémont [b], Jean-Michel Dogné [b,c], Bernard Pirotte [b], François Durant [a]

[a] *Département de Chimie, Laboratoire de Chimie Biologique Structurale, Facultés Universitaires Notre-Dame de la Paix, 61 rue de Bruxelles, B-5000 Namur, Belgium*
[b] *Natural and Synthetic Drugs Research Center, Laboratoire de Chimie Pharmaceutique, Université de Liège, 1 av. de l'Hôpital, tour 4(+5) Sart-Tilman, B-4000 Liège, Belgium*
[c] *Département de Pharmacie, Facultés Universitaires Notre-Dame de la Paix, 61 rue de Bruxelles, B-5000 Namur, Belgium*

Received 13 March 2006; received in revised form 7 July 2006; accepted 17 July 2006
Available online 9 October 2006

Abstract

A four-point pharmacophore of COX-2 selective inhibitors was derived from a training set of 16 compounds, using the Catalyst program. It consists of a H bond acceptor, two hydrophobic groups and an aromatic ring, in accordance with SAR data of the compounds and with topology of the COX-2 active site. This hypothesis, combined with exclusion volume spheres representing important residues of the COX-2 binding site, was used to virtually screen the Maybridge database. Eight compounds were selected for an in vitro enzymatic assay. Five of them show COX-2 inhibition close to that of nimesulide and rofecoxib, two reference COX-2 selective inhibitors. As a result, structure-based pharmacophore generation was able to identify original lead compounds, inhibiting the COX-2 isoform.

Keywords: COX-2 selective inhibitor; Structure-based pharmacophore; Virtual screening; Catalyst/HIPHOP; Hit identification

1. Introduction

Non-steroidal anti-inflammatory drugs (NSAIDs), like aspirin and indomethacin, are the most used agents worldwide, for example in the treatment of rheumatic diseases like osteo- and rheumatoid-arthritis or to relieve backache and headache [1–2]. However, most of these drugs lead to renal and gastrointestinal (GI) side-effects [3–4] causing about 70 000 hospitalizations and 7000 deaths per year in USA [5]. Development of new strategies to design potent anti-inflammatory drugs devoid of toxic effects is therefore essential.

Classical NSAIDs act by non-selective inhibition of cyclooxygenase (COX or prostaglandin endoperoxide H synthase) enzymes involved in the arachidonic cascade and catalyzing the biosynthesis of prostaglandins and thromboxane [6]. In the 1990s, a second isoform of COX termed COX-2 was discovered [7]. These two COX isoforms have two different modes of expression: the constitutive COX-1 with housekeeping functions (gastro-protection and keeping vascular and renal homeostasis) and the inducible COX-2, induced in pathological conditions by pro-inflammatory cytokines and playing a major role in inflammation, pain and fever [8–10]. Therefore, adverse GI effects of NSAIDs would be largely due to COX-1 inhibition [11]. As a result, the development of selective COX-2 inhibitors could provide anti-inflammatory drugs with fewer risks. Moreover, the COX-2 enzyme would be an interesting target in the treatment of some cancers [12–13] and neurodegenerative diseases like Alzheimer [14] and Parkinson [15]. Nimesulide (Mesulid®) [16] and celecoxib

* Corresponding author. Tel.: +32 81 72 54 57; fax: +32 81 72 45 30.
E-mail address: catherine.michaux@fundp.ac.be (C. Michaux).

0223-5234/$ - see front matter © 2006 Elsevier Masson SAS. All rights reserved.
doi:10.1016/j.ejmech.2006.07.017

(Celebrex®) [17] inhibit selectively COX-2 and are marketed for the treatment of arthritis and pain relief (Fig. 1). However, we have to mention that the biological functions of prostanoids are much more complex and interrelated than previously appreciated. Indeed, COX-2 is also constitutively expressed in some tissues including brain [18,19]. Moreover, recently, a third variant of the cyclooxygenase enzyme, COX-3, has been identified in the brain and was found to be composed of COX-1 and the retained intron. It was first considered as a potential target of paracetamol but final proof that its analgesic and antipyretic effects are dependent on COX is still lacking. Högestätt et al. propose an alternative mode of action for this compound [20]. Identification of COX-3 is opening a new chapter in inflammation and NSAID pharmacology [21,22].

At present, several chemical families of COX-2 inhibitors are developed in literature [23–25]. Their COX-2 selectivity mainly results from two structural differences between the two isoforms COX-1 and COX-2. Firstly, the substitution of Ile523 in COX-1 with the less bulky Val523 in COX-2 allows access to an additional hydrophilic side-pocket [26,27]. The existence of this one in COX-2 allows additional interactions with amino acids such as Arg513, replaced by a histidine in COX-1. This modification would be another contributor to COX-2 specificity [28]. Secondly, the conserved Leu384, located at the top of the channel, is oriented differently in the two isoforms. Indeed, in COX-1, the presence of a phenylalanine at position 503 forces the Leu384 side-chain to point into the active site. On the other hand, in COX-2, a smaller leucine at this position allows the Leu384 side-chain to move away from the active site and generates an accessible space in the apex of the COX-2 binding site [29]. These two main differences increase the volume of the COX-2 active site (20% larger) compared with the COX-1 one and could be used to design COX-2 selective inhibitors [30].

Currently, there is an ongoing research to design new COX-2 inhibitors structurally different from the current ones. Indeed, recently rofecoxib (Fig. 1), from the diaryl heterocycle family, was withdrawn from the market because of cardiotoxicity [31] which justifies that a constant effort is devoted to identify new scaffolds for the COX-2 inhibition.

In this paper, a pharmacophore model of 16 diverse and highly COX-2 selective inhibitors was generated, by using Catalyst/HIPHOP software, in order to identify new potential lead compounds. This hypothesis, combined with 44 exclusion volume spheres representing important amino acids of the human COX-2 binding site, was then used to screen *in silico* the 3D Maybridge database. Eight compounds were selected from the output hit list and their COX-2 inhibitory potency was preliminarily evaluated on a purified enzymatic assay.

2. Methods

2.1. Pharmacophore generation

Using Discover3 module [32] implemented in InsightII [33], conformational analysis was first performed for each selected COX-2 inhibitors (Fig. 2) in order to take into account their flexibility. The conformations optimized by molecular mechanics with the CFF91 forcefield were used as a starting point for the analysis. A simulated annealing procedure was then performed, running high temperature dynamics (1000 K for 2000 fs), followed by cooling down to 100 K with 1 fs molecular dynamics at each step. An energy minimization step was then followed using three algorithms: two first-order ones, the Steepest Descent (convergence criteria: 10 kcal mol^{-1} $Å^{-1}$) and Conjugate Gradient (0.01 kcal mol^{-1} $Å^{-1}$) and a second-order one, the Newton–Raphson (0.001 kcal mol^{-1} $Å^{-1}$). A distance dependent dielectric constant was chosen (1*r). For each compound, 100 conformers were generated and then clustered according to an RMSD (root mean square deviation; a measure of the average squared position difference between two equivalent atoms) of 0.5 Å. In addition, only in the case of **2**, the ESFF forcefield was used because the CFF91 one was not able to correctly model the azido function.

To perform hypothesis generation, Catalyst software and particularly the HIPHOP module was applied [34]. Unlike Catalyst/HYPOGEN, this algorithm identifies common features between compounds without considering activity. It takes a collection of conformational models of molecules and a selection of chemical groups, produces a series of molecular alignments and then identifies configurations of features that are common to the set of molecules. The hypotheses are ranked on the basis of the number of members fitting the pharmacophore and the frequency of its occurrence (Ranking score). The quality of the mapping between a compound and a hypothesis is indicated by the fit value. The Best Fit option manipulates the first 100 conformers within a specified energy threshold to minimize the distances between hypothesis features and mapped atoms in the molecule. As several applications show it, Catalyst is a useful tool for the discovery of new lead compounds for a given target [35–37].

Several chemical features are used including hydrogen bond acceptor/donor (A/D), hydrophobic group (H), ring aromatic (R) and negative/positive ionisable (N/P). Each

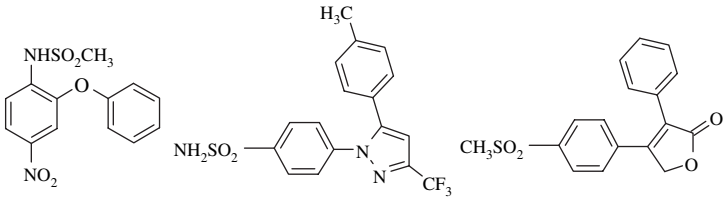

Nimesulide **Celecoxib** **Rofecoxib**

Fig. 1. Chemical structure of reference COX-2 selective inhibitors.

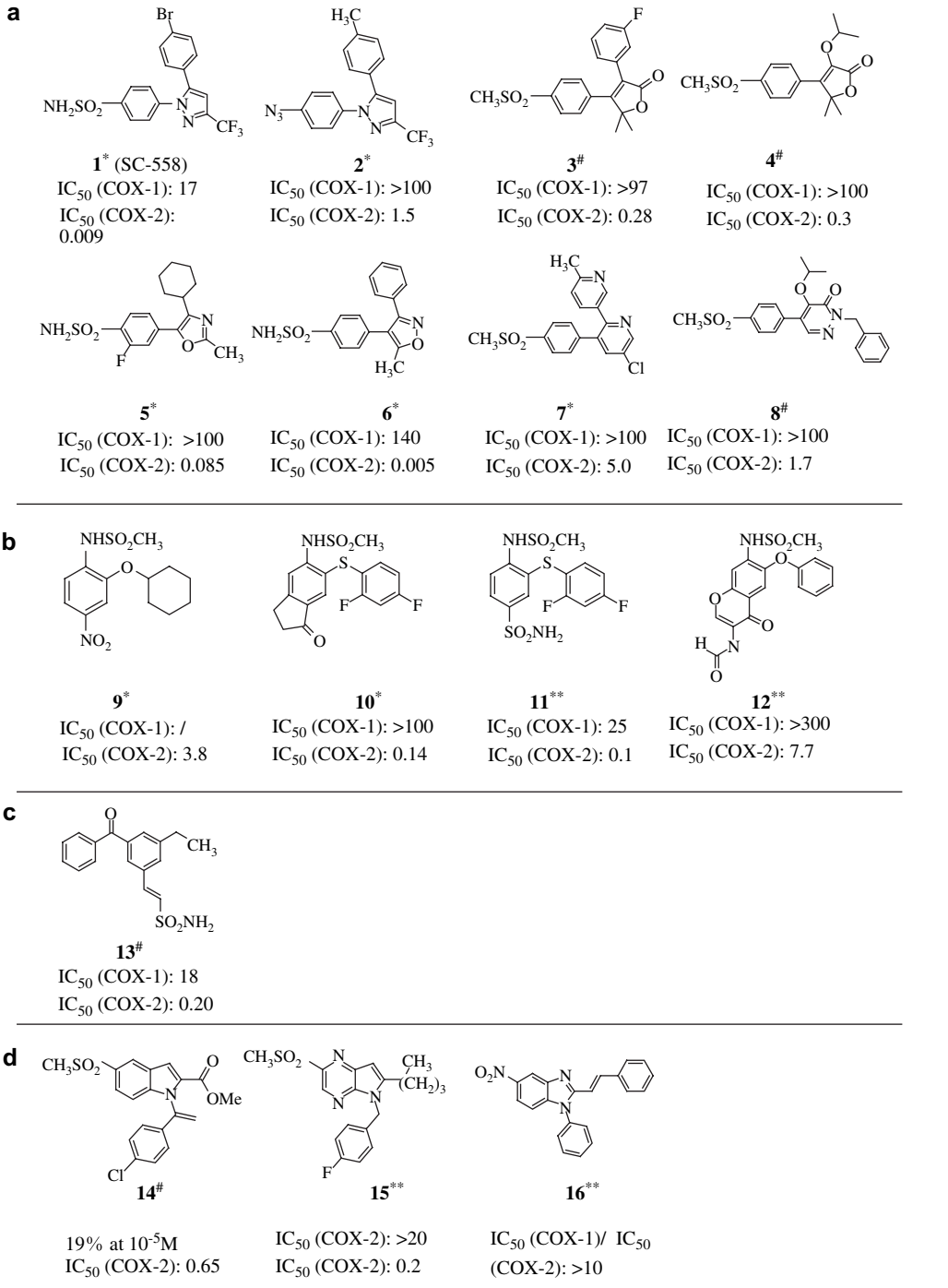

a: the diaryl heterocycle compounds; b: the sulphonamide derivatives; c: the analogues of flurbiprofen; d: the analogues of indomethacin
* Enzymatic assay
# Human whole blood assay
** Cellular assay

Fig. 2. Chemical structure of COX-2 selective inhibitors used as training set in the Catalyst/HIPHOP hypothesis generation. Activities are expressed in 10^{-6} M.

characteristic is located at a specific position and is surrounded by a spatial tolerance sphere of 1 Å radius. The A and D features are defined by two points: the heavy atom and the projected point of complementary site atoms. The resulting vector gives directionality to the hydrogen-bonding feature. The R feature, matching five- and six-member aromatic rings, also includes a vector with the ring centroid and a projected point normal to the ring plane.

The control parameters used for pharmacophore generation are summarized in Table 1.

In order to mimic the boundary of the human COX-2 active site and to take into consideration flexibility of the side-chains,

Table 1
Parameters used for running Catalyst hypothesis generation

Parameters	Value of the parameter	Definition of the parameter
Principal	2 for 1 1 for the others	All the chemical features in the compound will be considered in building hypothesis space At least one mapping for each generated hypothesis will be found
MaxOmit	0 for 1	Mapping of all features
Feat	1 for the others	All but one feature must map
Spacing	300 pm	Minimum distance between actual feature locations in molecules in the training set used for identifying candidate hypotheses
Minpoints	4	Minimum number of location constraints required for any hypotheses
MinSubset Points	4	Defining the regions of hypothesis space that are most likely to be relevant to the training set
Superposition Error	1	This option lets you adjust the rms fit of molecules to generated hypotheses. Reducing this value from 1 tightens the fit
Misses	1	This option means that hypotheses that fail to map completely to more than one training set compound will be disallowed
Feature Misses	1	Number of compounds allowed not to map any particular feature in a generated hypothesis
Mapping coefficient	0	This parameter controls the importance of having compounds with similar structure map to a hypothesis in a similar way

exclusion (ligand-inaccessible) volume spheres of 1.0 Å diameter were added to the selected 3D hypothesis, based on the human COX-2, modelled from crystallized murine COX-2 in complex with SC-558 (PDB code: 6COX) (data not shown). The spheres were set on the positions occupied by the side-chains of amino acids located at 10 Å from the active site centre. Such method could reduce the number of hits and also the number of false positives in a hit list by a factor of 2–5 [38].

2.2. Docking studies

The *Gold* docking program was used to select the hits resulting from the virtual screening and to emphasize the binding mode of the more potent leads, SPB04674 and BTB02472. *Gold* is a genetic algorithm for protein-ligand docking with full ligand and partial protein flexibility [39]. Indeed, conformations of some amino acids (Ser, Thr and Lys) are optimized during the run. The active site was defined as all protein atoms within 15 Å of any ligand atom in the experimental protein–ligand complex (6COX). It was adapted for the modelled human isoform. A maximum of 10 docking solutions were generated for each structure, with early termination of the process if the respective RMSDs of the three highest ranked docking solutions were within 1.5 Å RMSD of one another. The default software settings were used for the parameters controlling GOLD's genetic algorithm. A total of 100 000 genetic operations were carried out on five islands, each containing 100 individuals. The niche size was set to 2, and the value for the selection pressure was set to 1.1. Genetic operator weights for crossover, mutation, and migration were set to 95, 95 and 10, respectively. The scoring function used to rank the dockings was Goldscore. It is partly based on conformational and non-bonded contact information from the CSD database. It includes the terms for hydrogen-bonding, VDW, and intramolecular energies. The VDW interactions for the protein–ligand complex are described by a 8–4 potential. A 12–6 potential is used for the ligand steric energies that also include the torsion energies.

2.3. Pharmacological assay

As human COX-1 is not commercially available, the in vitro COX inhibitory assay was determined by using purified ovine COX enzymes supplied by Cayman Chemical Company. The ovine COX inhibitory activity was determined by measuring non-enzymatically PGE_2 production from arachidonic acid, substrate of COX enzymes [40]. The COX enzymes (1 unit consumes 1 O_2 nmol min^{-1} at 37 °C in 0.1 M Tris–HCl pH 8, 2×10^{-3} M phenol, 1×10^{-6} M hematin and 1×10^{-4} M arachidonic acid) were first incubated with drugs (diluted in 0.2–1% DMSO) for 1 h in their optimal activity conditions: pH 8, 37 °C and with two cofactors (hematin and phenol). Then 0.1 ml of sodium arachidonate (10^{-5} mol L^{-1}) was added and incubation continued for 2 min. The enzymatic reaction was stopped by adding 0.1 ml of diclofenac (potent non-selective COX inhibitor, 10^{-3} M) and putting samples in ice. The solutions were then diluted 10× in Tris–HCl buffer and PGE_2 production was measured by radio-immuno assay.

3. Results and discussion

3.1. Pharmacophore generation

Pharmacophore models of COX-2 selective inhibitors are already described in the literature but were established from a not very diverse training set [41–47]. To set up a more general pharmacophore, a larger structural diversity was taken into account. Moreover, pharmacophore generation requires compounds with potentially the same binding orientation in the active site. As described previously [25], four classes of inhibitors were shown to fill the hydrophilic pocket specific to

COX-2 and exhibit therefore the same binding mode. These are (a) the diaryl heterocycle compounds, (b) the sulphonamide derivatives and, (c) the analogues of flurbiprofen and (d) indomethacin. Among them, 16 highly COX-2 selective molecules were selected as a training set for the pharmacophore analysis (Fig. 2) [23,25,42,48–61]. Compound **1**, SC-558, an analogue of celecoxib, is the only COX-2 selective inhibitor to be co-crystallized with COX-2 isoform (6COX) [26]. Analogues of rofecoxib, **3** and **4**, and, analogue of nimesulide, **9**, were preferred to their parents because of their better COX-2 selectivity.

A conformational analysis was performed on each molecule to assess their flexibility and to determine their low-energy conformations and among them, their bioactive one. The energy range of the conformers generated for each compound (ΔE: energy difference between lowest and highest energy conformer) and the maximal RMSD between any two conformers are depicted in Table 2. The co-crystallized conformation of **1** was considered as the bioactive one and no conformational model was performed for this molecule. The generated conformers of each inhibitor were checked against experimental analogue structures observed in the CSD database, when available (data not shown).

The molecules with their full conformational model were then submitted to the Catalyst hypothesis generation. HIPHOP module of Catalyst was used because in some families, not enough biological data are available. **1** was chosen as a reference compound (Principal = 2; MaxOmitFeat = 0). It was allowed to map all features although the others were allowed to map partially on the hypotheses (Principal = 1; MaxOmitFeat = 1). The 10 generated models consist of three or four points (Table 3). The last hypotheses (h6 to h10) are less specific than the others because they only have three points and were not retained. The four-point hypothesis h5 is characterized by two H bond acceptors, an aromatic ring and a hydrophobic group. 2D mapping of **1** on this pharmacophore is depicted in Fig. 3. This model is not in agreement with SAR of the diaryl heterocycle family. Indeed, nitrogen of the pyrazole cycle in **1** is not involved in hydrogen-bonding with residues of the COX-2 active site (6COX) [26]. Moreover, the essential role of the central ring of diaryl heterocycle compounds is only to orientate correctly the two phenyl groups in the binding site [62]. On the other hand, the first four hypotheses[1] (h1 to h4) displaying a H bond acceptor (A), an aromatic ring (R) and two hydrophobic groups (H) are in good agreement with SAR data. 3D mapping of **1** and 2D mapping of **9**, **13**, **15** and **16** on the first hypothesis are depicted in Fig. 4 by way of illustration. Each compound of the training set shows a good best fit value with the pharmacophore model.

3.2. Reliability of the generated pharmacophore

The first hypothesis is reliable because it corroborates the SAR for the different inhibitors and fits the COX-2 active site. In the diaryl heterocycle family, replacement of sulfonamide or sulfone group by hydrogen or chlorine atom leads to COX-1 selective compounds [17]. Moreover, interactions between the sulfonamide moiety of **1** and polar amino acids of the hydrophilic pocket, specific to COX-2 are observed in the crystallized complex (6COX) [30]. H bond acceptor feature is therefore essential for COX-2 selectivity. The hydrophobic group, corresponding to CF_3 group in **1**, seems important because when substituted by a polar group like CH_2OH or $CONH_2$, the COX-2 inhibition is reduced [17]. Few SAR data are available in literature for the sulfonamide family but the withdrawing group (nitro, sulfonamide,…), reflected by feature A, seems to be necessary [56,60–61]. Introduction of hydrogen, cyano or alcohol substituents instead of an ethyl group (hydrophobic group) in **13**, lowered COX-2 inhibitory activity and selectivity [42]. In addition, the length of the chain bearing the sulfonamide group (and thus position of sulfonamide moiety) is also important [42]. The analogue compound of **14**, with a carboxylic acid group in place of the ester one, shows no cyclooxygenase inhibition [41]. As a result, the methyl group of **14**, corresponding of one of the two hydrophobic groups (H), seems important for activity. Few SAR data exist for compounds **15** and **16**.

Comparison of the hypothesis with complex of **1** in COX-2 isoenzyme shows the pharmacophore and COX-2 binding site

Table 2
Number of conformers, ΔE and RMSD values for each compound

Compound	Number of conformers	ΔE (kcal mol^{-1})	RMSD max (Å)
2	16	0.04	3.35
3	16	0.31	1.76
4	12	4.22	1.90
5	7	2.17	1.27
6	16	0.01	1.85
7	15	1.66	1.84
8	55	2.19	3.08
9	48	4.44	2.00
10	30	7.96	2.38
11	43	4.50	2.92
12	44	6.81	2.28
13	70	2.55	3.61
14	31	0.96	2.54
15	27	2.92	2.13
16	38	8.30	2.70

Table 3
Results of the common-feature hypothesis run

Hypothesis	Molecular features	Ranking score
h1	ARHH	110.6
h2	ARHH	110.6
h3	ARHH	110.2
h4	ARHH	110.2
h5	AARH	102.4
h6	ARH	92.8
h7	ARH	92.8
h8	ARH	92.8
h9	ARH	86.9
h10	ARH	86.9

A, hydrogen bond acceptor; R, ring aromatic; H, hydrophobic group.

[1] The difference between each hypothesis lies in the orientation of the projected point of the H bond acceptor and the aromatic ring.

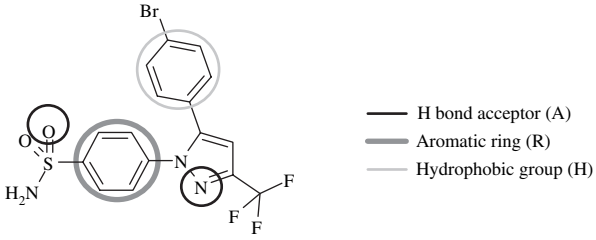

Fig. 3. 2D mapping of **1** on the fifth hypothesis.

complement each other. The hydrogen acceptor (A) is located in the specific hydrophilic side-pocket; the two hydrophobic groups (H) are at the top and at the bottom of the hydrophobic channel, respectively, while the aromatic ring (R) sits at the entrance of the side-pocket (Fig. 5).

The generated hypothesis is quite different from the other pharmacophores described elsewhere. Indeed, these ones either have only three pharmacophore points [41–42,46], or have a second H bond acceptor as in the hypothesis h5 [43–45,47].

This study highlights the importance and the role of traditional SAR and its complementarity with data coming from computerized pharmacophore.

3.3. Virtual screening from a structure-based pharmacophore

In this study, pharmacophore-based screening was applied because it is much faster than docking. The usefulness of feature-based pharmacophore as queries for successful 3D database search has recently been reviewed [63]. Nevertheless,

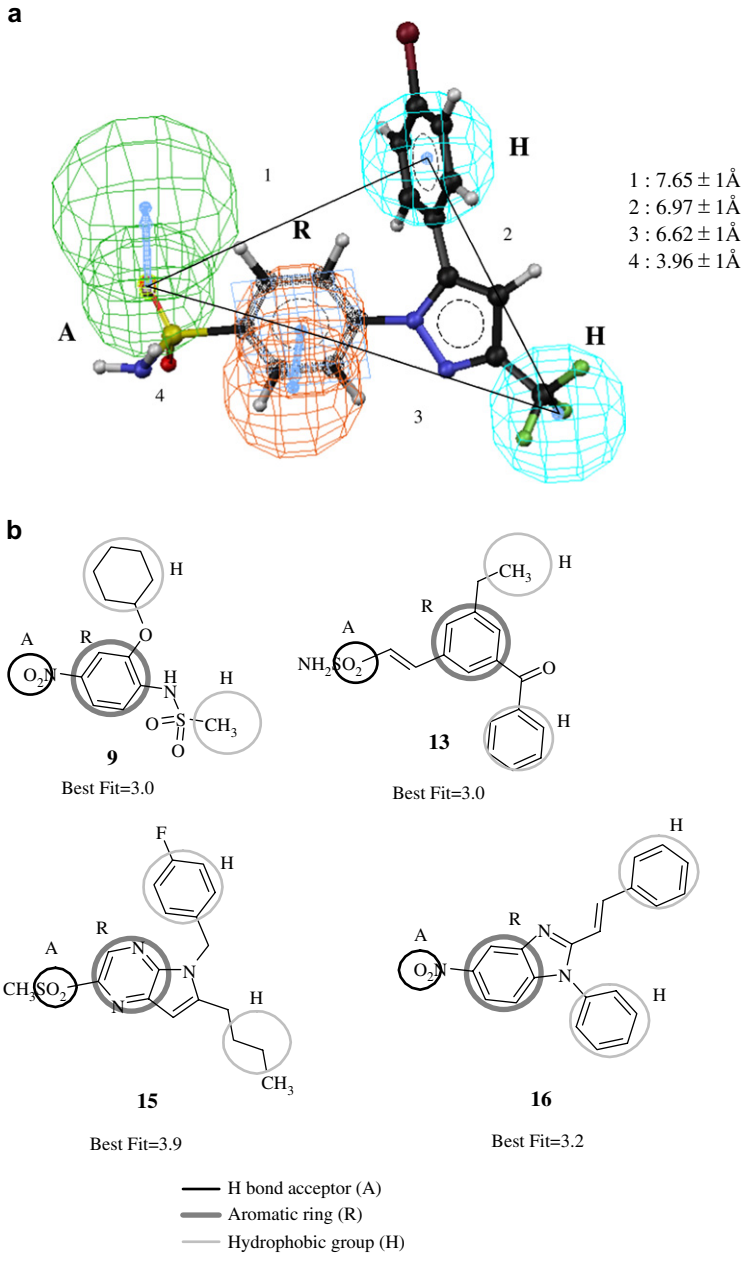

Fig. 4. a) 3D mapping of **1** on the first hypothesis; b) 2D mapping of **9**, **13**, **15**, and **16** on the first hypothesis.

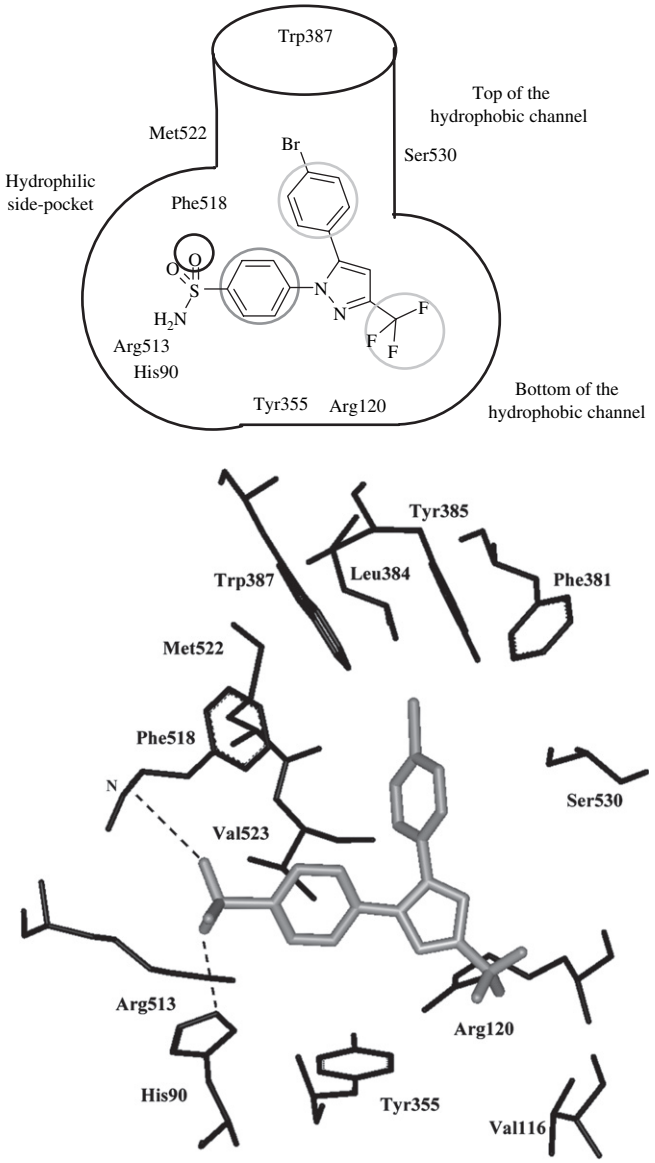

Fig. 5. Human COX-2 active site in complex with **1** mapping the four features of the generated pharmacophore.

in order to be more specific to the human COX-2 binding site, 44 exclusion volume spheres, representing the important amino acids, were added to the model. Structure-based pharmacophores were shown to be as accurate as docking [64].

The Maybridge database was searched using the ''Fast Flexible Search Databases'' algorithm which only uses the precomputed conformations of compounds during the search. The 44 exclusion volume spheres enabled to shrank the Maybridge hit list from 12 675 to 2577, i.e. a factor of 5.

The first 300 hits fitting the model were selected for further analyses. In order to reduce the number of molecules to test, several selection criteria were used. An initial filtering to satisfy the Lipinski rules was first applied to the compounds: MW < 500, log $P < 5$, number of H acceptors <10 and number of H donors <5 [65]. As a next step, hits with asymmetric carbon(s) were omitted to simplify the problem. Indeed, most compounds of the Maybridge database are commercially available in racemic mixture which would have to be separated. Moreover, to avoid too flexible compounds, those with more than seven rotatable bonds were rejected [66].

In a final step, the 135 remaining hits were first docked into the human modelled COX-2 active site using GOLD program in order to take into account molecular complementarities between the compounds and the COX-2 enzyme. The binding modes were ranked according to the scoring function (called ''Fitness'') of GOLD. Secondly, the Catalyst ''Best Fit'' scoring was calculated for each hit, reflecting the mapping of the compound in the hypothesis. The compounds with ''Fitness'' <40 and ''Best Fit'' <1 were rejected. From these analyses, 40 best-scored molecules still remained. Visual inspection of the suggested binding modes of GOLD, together with the high scoring values of GOLD and Catalyst, were used to select eight structures for in vitro testing (Fig. 6). For these ones, the H bond acceptor feature is a carbonyl, ether or a nitro group. The hydrophobic groups match an aliphatic group, a halogen, a phenyl or an aliphatic ring.

3.4. Pharmacological assay: identification of original molecules

With the goal to identify new leads having a preferential action on the enzyme COX-2, the enzymatic assay is by far the best choice for the first step in a drug design process. Even if it has limitations in comparison with a cellular assay (for example, in this case, no membrane environment), it can emphasize unambiguously the specific drug–enzyme interaction [40]. As human COX-1 is not commercially available, purified ovine COXs were first used in order to determine COX-1/COX-2 selectivity of the selected compounds. Ovine and human COX species show 80–90% sequence identity and their binding sites are strictly identical [67]. It is therefore assumed that the structure–activity/selectivity relationships would show the same trends in a human COX-1 and COX-2 assays.

In this paper, a screening assay was first performed at 10^{-5} M concentration in order to identify potential original lead compounds (Table 4). Reference COX-2 inhibitors, as nimesulide, rofecoxib and celecoxib, were also tested and compared to the new molecules. As shown in Table 4, their activity values are weak in comparison with others carried out by different assays (i.e. human whole blood assay), but are valid and relevant. Indeed, the used method was validated and showed consistent results [40,67]. The previously reported gradation in the inhibitor potency for different reference drugs is respected by our assay; i.e. rofecoxib is more potent and selective than nimesulide. Moreover, it was clearly demonstrated in literature that the measured COX's inhibitory potency of NSAIDs can strongly vary depending on the evaluation conditions (incubation time, arachidonic acid concentration, etc.) [68].

While three test candidates are inactive, five of them show a significant COX-2 activity, close to the one of nimesulide, and preferentially inhibit the COX-2 isoform. Particularly, SPB04674 and BTB02472 are as potent as rofecoxib and have a new scaffold in comparison with reference inhibitors and all others proposed in literature. Both compounds were

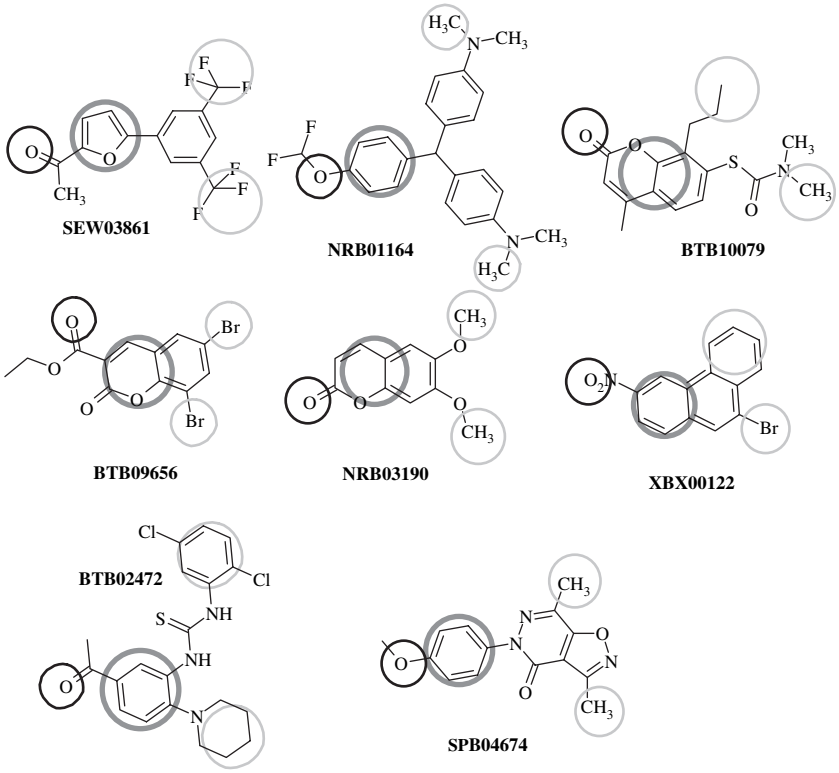

Fig. 6. 2D mapping of the eight selected compounds on the first hypothesis.

docked in the human COX-2 binding site (using GOLD program) and showed a good complementarity with the isoform. In the case of BTB02472, the carbonyl group interacts by hydrogen-bonding with amino acids of the hydrophilic pocket, and particularly His90. This interaction is shown to be important in the complex of **1** in COX-2. Moreover, the piperidine and dichlorophenyl groups lie, respectively, at the bottom and at the top of the hydrophobic channel (Fig. 7). CH···π interaction is observed between Tyr355 and the piperidine moiety. The dichlorophenyl group is surrounded by aromatic residues like Trp387, Phe381 and Tyr385. For SPB04674 (data not shown), the ether group is H bonded with His90 and both methyl bind in the hydrophobic channel. Moreover, H bond is observed between the pyridazinone carbonyl and Tyr355. This is an additional interaction in comparison with the proposed pharmacophore.

For the three inactive compounds, their pharmacological profile is understandable. Indeed, in the case of BTB10079 and NRB01164, the hypothesized H bond acceptor is not binding the hydrophilic pocket and no H bond is observed. Actually, in BTB10079, the amide group, and not the expected coumarinic carbonyl, is in the hydrophilic pocket where no special interaction is observed. In the case of NRB01164, this is one of the amine groups, and not the ether, which binds the polar pocket. For SEW03861, the bottom of the channel is not enough filled as compared with SPB04674 which makes more contacts with the enzyme.

Such results show that the proposed pharmacophore cannot reproduce the subtle interactions inside the COX-2 active site but can anyway test our COX-2 structure-based pharmacophore model from which we are able to identify potential COX-2 inhibitor. The new structures are original and are not members of known families of COX-2 inhibitors. Therefore, they are promising candidates for further structural modifications which could lead to more potent COX-2 selective inhibitors. Further studies will have to be performed in order to optimize these new structures. It will be, for example, interesting, as a second step, to test the best candidates in a human whole blood assay which is a much more robust assay because of reflecting more the complexity of the physiological environment.

Table 4
In vitro activities of eight compounds identified from virtual screening

Compound	% COX-1 inhibition (10^{-5} M)[a]	% COX-2 inhibition (10^{-5} M)[a]
SEW03861	i	i
NRB01164	i	i
BTB10079	i	i
BTB09656	i	12.30 ± 5.00
NRB03190	i	16.65 ± 3.51
XBX00122	i	17.14 ± 11.24
BTB02472	5.10 ± 3.00	26.36 ± 6.69
SPB04674	i	33.85 ± 12.70
Nimesulide	9.87 ± 3.55	19.94 ± 2.78
Rofecoxib	i	24.51 ± 2.19
Celecoxib	12.35 ± 10.04	40.37 ± 3.79

i: inactive compound.
[a] Average of three determinations.

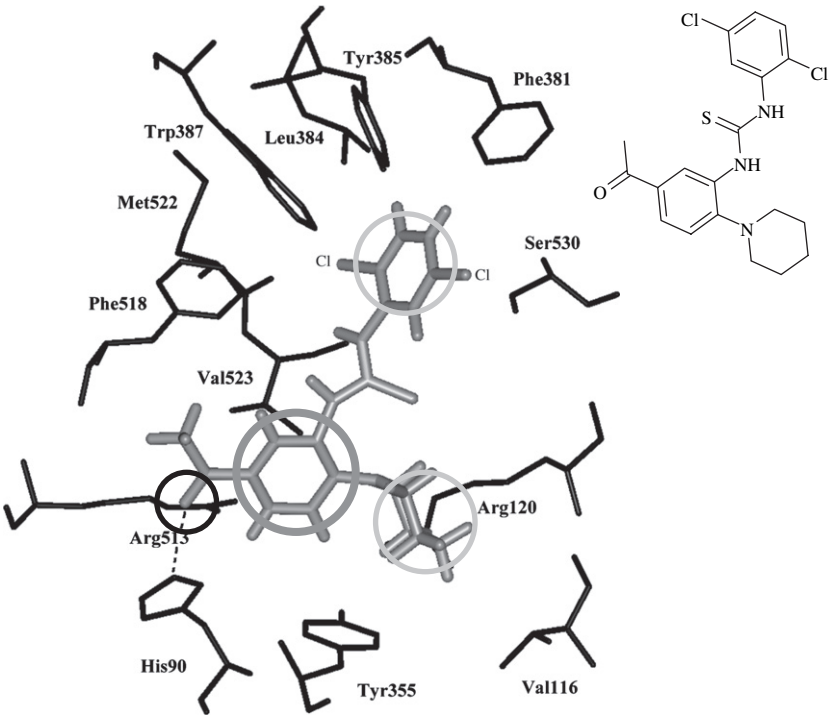

Fig. 7. Human COX-2 active site in complex with BTB02472.

4. Conclusions

In order to identify new lead COX-2 inhibitors, a 3D pharmacophore model was generated from Catalyst/HIPHOP program, using a training set of 16 COX-2 selective inhibitors. The selected hypothesis consists of a H bond acceptor, responsible of COX-2 selectivity, two hydrophobic groups and an aromatic ring. Such model is in good agreement with SAR data and characteristics of COX-2 active site. In order to take into account topology of the human COX-2 binding site, 44 exclusion volume spheres were added to the hypothesis and the structure-based pharmacophore was used as a 3D query to screen the Maybridge 3D database. The first 300 hits were then selected for further analysis. From biodisponibility, scoring and flexibility criteria, 40 compounds were retained and eight were assayed on the basis of their high scoring values. Five of them preferentially inhibit COX-2 and two of them have a pharmacological profile similar to rofecoxib, a potent COX-2 selective compound, and have an original scaffold. Therefore, Catalyst-generated pharmacophore model and enzymatic assay were useful in the identification of potential COX-2 selective original lead compounds.

Acknowledgments

Catherine Michaux acknowledges the Fonds National de la Recherche Scientifique (FNRS) for financial support. This work was also supported by grant of the French Community of Belgium (no. 99/04-249).

References

[1] J.J. Dubost, M. Soubrier, B. Sauvezie, Rev. Med. Interne. 20 (1999) 171–178.
[2] W.D. Blackburin, Am. J. Med. 100 (1996) 24S–30S.
[3] B. Cryer, M.B. Kimmey, Am. J. Med. 105 (1998) 20S–30S.
[4] A. Whelton, Am. J. Med. 106 (1999) 13S–24S.
[5] P. Eschwège, V. de Ledinghen, T. Camilli, S. Kulkarni, G. Dalbagni, S. Droupy, A. Jardin, G. Benoît, B.B. Weksler, Presse Med. 30 (2001) 508–517.
[6] J.R. Vane, Nat. N. Biol. 231 (1971) 232–235.
[7] M.J. Holtzman, J. Turk, L.P. Shornick, J. Biol. Chem. 267 (1992) 21438–21445.
[8] J.Y. Fu, J.L. Masferrer, K. Seibert, A. Raz, P.J. Needleman, Biol. Chem. 265 (1990) 16737–16740.
[9] L.J.J. Crofford, Rheumatology 24 (Suppl. 49) (1997) 15–19.
[10] A. Ristimaki, S. Garfinkel, J. Wessendorf, T. Maciag, T. Hla, J. Biol. Chem. 269 (1994) 11769–11775.
[11] F.L. Lanza, Scand. J. Gastroenterol. 163 (Suppl.) (1989) 24–31.
[12] K. Subbaramaiah, A.J. Dannenberg, Trends Pharmacol. Sci. 24 (2003) 96–102.
[13] M.A. Iniguez, A. Rodriguez, O.V. Volpert, M. Fresno, J.M. Redondo, Trends Mol. Med. 9 (2003) 73–78.
[14] Z. Xiang, L. Ho, J. Valdellon, D. Borchelt, K. Kelley, L. Spielman, P.S. Aisen, G.M. Pasinetti, Neurobiol. Aging 23 (2002) 327–334.
[15] Z.H. Feng, T.G. Wang, D.D. Li, P. Fung, B.C. Wilson, B. Liu, S.F. Ali, R. Langenbach, J.S. Hong, Neurosci. Lett. 329 (2002) 354–358.
[16] I.A. Tavares, P.M. Bishai, A. Bennett, Arzneimittelforschung 45 (1995) 1093–1095.
[17] T.D. Penning, J.J. Talley, S.R. Bertenshaw, J.S. Carter, P.W. Collins, S. Docter, M.J. Graneto, L.F. Lee, J.W. Malecha, J.M. Miyashiro, R.S. Rogers, D.J. Rogier, S.S. Yu, G.D. Anderson, E.G. Burton, J.N. Cogburn, S.A. Gregory, C.M. Koboldt, W.E. Perkins, K. Seibert, A.W. Veenhuizen, Y.Y. Zhang, P.C. Isakson, J. Med. Chem. 40 (1997) 1347–1365.
[18] L. Parente, M. Perretti, Biochem. Pharmacol. 65 (2003) 153–159.

[19] C.D. Breder, D. Dewitt, R.P. Kraig, J. Comp. Neurol. 355 (1995) 296–315.
[20] E.D. Högestätt, B.A.G. Jönsson, A. Ermund, D.A. Andersson, H. Björk, J.P. Alexander, B.F. Cravatt, A.I. Basbaum, P.M. Zygmunt, J. Biol. Chem. 280 (2005) 31405–31412.
[21] S.S. Shaftel, J.A. Olschowka, S.D. Hurley, A.H. Moore, M.K. O'Banion, Brain Res. Mol. Brain Res. 119 (2003) 213–215.
[22] N.V. Chandrasekharan, H. Dai, K.L. Roos, N.K. Evanson, J. Tomsik, T.S. Elton, D.L. Simmons, Proc. Natl. Acad. Sci. U.S.A. 19 (2002) 19.
[23] C.J. Hawkey, Lancet 353 (1999) 307–314.
[24] A.S. Kalgutkar, Exp. Opin. Ther. Patents 9 (1999) 831–849.
[25] C. Michaux, C. Charlier, Mini Rev. Med. Chem. 4 (2004) 603–615.
[26] R.G. Kurumbail, A.M. Stevens, J.K. Gierse, J.J. McDonald, R.A. Stegeman, J.Y. Pak, D. Gildehaus, J.M. Miyashiro, T.D. Penning, K. Seibert, P.C. Isakson, W.C. Stallings, Nature 384 (1996) 644–648.
[27] J.K. Gierse, J.J. McDonald, S.D. Hauser, S.H. Rangwala, C.M. Koboldt, K.J. Seibert, Biol. Chem. 271 (1996) 15810–15814.
[28] E. Wong, C. Bayly, H.L. Waterman, D. Riendeau, J.A. Mancini, J. Biol. Chem. 272 (1997) 9280–9286.
[29] C.I. Bayly, W.C. Black, S. Léger, N. Ouimet, M. Ouellet, M.D. Percival, Bioorg. Med. Chem. Lett. 9 (1999) 307–312.
[30] C. Luong, A. Miller, J. Barnett, J. Chow, C. Ramesha, M.F. Browner, Nat. Struct. Biol. 3 (1996) 927–933.
[31] C.A. Thompson, Am. J. Health. Syst. Pharm. 61 (2004) 2234–2236 2238.
[32] Accelrys Inc., Discover3, Version 2.98 ed., San Diego, 1998.
[33] Accelrys Inc., InsightII, San Diego, 2000.
[34] Accelrys Inc., Catalyst, Version 4.6 ed., San Diego, 2000.
[35] C. Michaux, J.M. Dogne, S. Rolin, B. Masereel, J. Wouters, F. Durant, Eur. J. Med. Chem. 38 (2003) 703–710.
[36] A. Hirashima, M. Morimoto, E. Kuwano, E. Taniguchi, M. Eto, J. Mol. Graphics Mod. 21 (2002) 81–87.
[37] Biogen Inc. (P. Sprague, Z. Zheng, S.P. Adams, A. Castro, J. Singh, H. Van Vlijmen), Molecular model for VLA-4 inhibitors US6552216, 2003.
[38] P.A. Greenidge, B. Carlsson, L.-G. Bladh, M. Gillner, J. Med. Chem. 41 (1998) 2503–2512.
[39] Gold Version 1.2 ed., Astex Technology, Cambridge, UK, 2001
[40] X. de Leval, J. Delarge, P. Devel, P. Neven, C. Michaux, B. Masereel, B. Pirotte, J.L. David, Y. Henrotin, J.M. Dogné, Prostaglandins Leukot. Essent. Fatty Acids 64 (2001) 211–216.
[41] A. Palomer, F. Cabre, J. Pascual, J. Campos, M.A. Trujillo, A. Entrena, M.A. Gallo, L. Garcia, D. Mauleon, A. Espinosa, J. Med. Chem. 45 (2002) 1402–1411.
[42] A. Palomer, J. Pascual, M. Cabre, L. Borra's, G. Gonzalez, M. Aparici, A. Carabaza, F. Cabre, M.L. Garcija, D. Mauleon, Bioorg. Med. Chem. Lett. 12 (2002) 533–537.
[43] C.R. Rodrigues, M.P. Veloso, H. Verli, C.A. Fraga, A.L. Miranda, E.J. Barreiro, Curr. Med. Chem. 9 (2002) 849–867.
[44] S. Prasanna, E. Manivannan, S.C. Chaturvedi, Biorg. Med. Chem. Lett. 14 (2004) 4005–4011.
[45] J.M. Rollinger, S. Haupt, H. Stuppner, T.J. Langer, J. Chem. Inf. Comput. Sci. 44 (2004) 480–488.
[46] J.J. Sutherland, L.A. O'Brien, D.F. Weaver, J. Med. Chem. 47 (2004) 3777–3787.
[47] S. Renner, G. Schneider, J. Med. Chem. 47 (2004) 4653–4664.
[48] A.G. Habeeb, P.N. Praveen Rao, E.E. Knaus, J. Med. Chem. 44 (2001) 3039–3042.
[49] D. Riendeau, M.D. Percival, S. Boyce, C. Brideau, S. Charleson, W. Cromlish, D. Ethier, J. Evans, J.P. Falgueyret, A.W. Ford-Hutchinson, R. Gordon, G. Greig, M. Gresser, J. Guay, S. Kargman, S. Leger, J.A. Mancini, G. O'Neill, M. Ouellet, I.W. Rodger, M. Therien, Z. Wang, J.K. Webb, E. Wong, C.C. Chan, Br. J. Pharmacol. 121 (1997) 105–117.
[50] Y. Leblanc, P. Roy, S. Boyce, C. Brideau, C.C. Chan, S. Charleson, R. Gordon, E. Grimm, J. Guay, S. Léger, C.S. Li, D. Riendeau, D. Visco, Z. Wang, J. Webb, L.J. Xu, P. Prasit, Bioorg. Med. Chem. Lett. 9 (1999) 2207–2212.
[51] K. Wakitani, T. Nanayama, M. Masaki, M. Matsushita, Jpn. J. Pharmacol. 78 (1998) 365–371.
[52] J.J. Talley, D.L. Brown, J.S. Carter, M.J. Graneto, C.M. Koboldt, J.L. Masferrer, W.E. Perkins, R.S. Rogers, A.F. Shaffer, Y.Y. Zhang, B.S. Zweifel, K. Seibert, J. Med. Chem. 43 (2000) 775–777.
[53] D. Riendeau, M.D. Percival, C. Brideau, S. Charleson, D. Dube, D. Ethier, J.P. Falgueyret, R.W. Friesen, R. Gordon, G. Greig, J. Guay, J. Mancini, M. Ouellet, E. Wong, L. Xu, S. Boyce, D. Visco, Y. Girard, P. Prasit, R. Zamboni, I.W. Rodger, M. Gresser, A.W. Ford-Hutchinson, R.N. Young, C.C. Chan, J. Pharmacol. Exp. Ther. 296 (2001) 558–566.
[54] Merck Frosst Canada, Inc. (C.K. Lau, C.S. Li, M. Therien, J.Y. Gauthier, P. Prasit), Pyridazinones as inhibitors of cyclooxygenase-2 WO9841511, 1998.
[55] N. Futaki, S. Takahashi, M. Yokoyama, I. Arai, S. Higuchi, S. Otomo, Prostaglandins 47 (1994) 55–59.
[56] N. Ouimet, C.C. Chan, S. Charleson, D. Claveau, R. Gordon, D. Guay, C.S. Li, M. Ouellet, D.M. Percival, D. Riendeau, E. Wong, R. Zamboni, P. Prasit, Bioorg. Med. Chem. Lett. 9 (1999) 151–156.
[57] Nycomed Austria GMBH (H. Blaschke, H. Fellier, F. Rovenszky, M. Hartmann, P. Kremminger, D. Stimmeder), Substituted derivatives of benzosulphonamides as inhibitors of the enzyme cyclooxygenase II WO9833769, 2001.
[58] K. Tanaka, H. Kawasaki, K. Kurata, Y. Aikawa, Y. Tsukamoto, T. Inaba, Jpn. J. Pharmacol. 67 (1995) 305–314.
[59] Pfizer (US) (Y. Okumura, T. Mano, R.W. Stevens), Benzimidazole compounds EP0846689, 1998.
[60] A.S. Lages, K.C. Silva, A.L. Miranda, C.A. Fraga, E.J. Barreiro, Bioorg. Med. Chem. Lett. 8 (1998) 183–188.
[61] C.S. Li, W.C. Black, C.C. Chan, A.W. Ford-Hutchinson, J.-Y. Gauthier, R. Gordon, D. Guay, S. Kargman, C.K. Lau, J. Mancini, N. Ouimet, P. Roy, P. Vickers, E. Wong, R.N. Young, R. Zamboni, P. Prasit, J. Med. Chem. 38 (1995) 4897–4905.
[62] D.B. Reitz, J.J. Li, M.B. Norton, E.J. Reinhard, J.T. Collins, G.D. Anderson, S.A. Gregory, C.M. Koboldt, W.E. Perkins, K. Seibert, P.C. Isakson, J. Med. Chem. 37 (1994) 3878–3881.
[63] T. Langer, E.M. Krovat, Curr. Opin. Drug Discov. Dev. 6 (2003) 370–376.
[64] J.S. Mason, A.C. Good, E.J. Martin, Curr. Pharm. Des. 7 (2001) 567–597.
[65] C.A. Lipinski, F. Lombardo, B.W. Dominy, P.J. Feeney, Adv. Drug Deliv. Rev. 46 (2001) 3–26.
[66] D.F. Veber, S.R. Johnson, H.Y. Cheng, B.R. Smith, K.W. Ward, K.D. Kopple, J. Med. Chem. 45 (2002) 2615–2623.
[67] C. Michaux, C. Charlier, F. Julemont, X. de leval, J.M. Dogne, B. Pirotte, F. Durant, Eur. J. Med. Chem. 40 (2005) 1316–1324.
[68] J.K. Gierse, C.M. Koboldt, M.C. Walker, K. Seibert, P.C. Isakson, Biochem. J. 339 (1999) 607–614.